Desalination and Water Treatment
www.deswater.com

doi: 10.5004/dwt.2019.24489

166 (2019) 334–343
October

Removal efficiency and mechanisms of dissolved Cr(VI) using oak wood biochar

Na Liu[a], Yuting Zhang[a], Peng Liu[b], Jing Lv[a], YingYing Liu[c,*], Longzhen Ding[a], Yadong Yang[a]

[a]*Key Laboratory of Groundwater Resources and Environment, Ministry of Education, College of Environment and Resources, Jilin University, Changchun 130021, China, emails: liuna@jlu.edu.cn (N. Liu), 986780134@qq.com (Y. Zhang), 594763747@qq.com (J. Lv), dinglz16@mails.jlu.edu.cn (L. Ding), yangyadong9@126.com (Y. Yang)*
[b]*School of Environmental Studies, China University of Geosciences, 388 Lumo Rd., Wuhan, Hubei 430074, PR China, email: liupeng5182@gmail.com*
[c]*Department of Earth and Environmental Sciences, University of Waterloo, Waterloo, Ontario, Canada N2L 3G1, email: yy4liu@uwaterloo.ca*

Received 5 January 2019; Accepted 3 June 2019

ABSTRACT

Environmental chromium (Cr) contamination has led to serious problems in the ecosystem owning to the carcinogenicity, toxicity, and teratogenicity of Cr. In this study, the latent application of oak wood biochar for dissolved Cr(VI) removal was investigated. Optimal treatment of Cr(VI) was achieved with a removal efficiency of 99.9% at a pH 2.0. Another critical factor influencing removal efficiency was the initial concentration of Cr(VI). The removal efficiency of Cr(VI) was >99.9% at 1–50 mg L^{-1}; nevertheless, Cr(VI) removal rate decreased at Cr(VI) concentrations (50–600 mg L^{-1}). Five kinetic equations were used to describe the Cr(VI) removal kinetics and the best fit was the pseudo-second-order model. Fourier transform infrared spectroscopy results showed that C–O groups of alcohol and C=O bonds may participate in the reaction. X-ray photoelectron spectroscopy analysis demonstrated that Cr is predominantly excited as Cr(III) species (~82.96%). The increase in pH values and concentrations of the cations Ca^{2+}, Na^{+}, and K^{+} in the aqueous solution after the reaction indicated that ion exchange was likely responsible for Cr(III) binding with the biochar. Results indicated that the electrostatic force between $Cr_2O_7^{2-}$ and biochar, Cr(VI) reduction by C–O groups in alcohol, and ion exchange and complexation between Cr(III) and C=O were the reaction mechanism.

Keywords: Removal mechanism; Cr(VI); Biochar; Cr(III); Kinetics

1. Introduction

Pollution by chromium (Cr) creates serious problems on human health. The major sources of environmental Cr contamination are related to the release of wastewater from electroplating, leather tanning, electroplating chemical manufacturing, and wood preservation [1,2]. Cr(III) and Cr(VI) are two primary species with contrary properties [3]. Cr(III) possesses less toxicity and mobility, but more stability than Cr(VI). $Cr_2O_7^{2-}$ is the predominant form with high Cr concentration and a low pH, however, Cr(VI) exits as CrO_4^{2-} when pH > 6.5 [4,5]. Exposure to Cr(VI) in the environment can lead to a variety of diseases affecting human health and the ecosystem. Therefore, US EPA recommends limiting the concentration of toxic Cr(VI) to 0.05 mg L^{-1} [6].

Common Cr(VI) treatment methods include ultrafiltration, membrane separation, chemical precipitation, reverse osmosis, and ion exchange [7–11]. However, the cost ineffectiveness,

* Corresponding author.

energy inefficiency, and limited metal removal [5] restrict the large-scale application of these treatments. Biochar produced via oxygen-free pyrolysis of biomass has been widely investigated and applied for treating Cr(VI)-polluted aqueous environments because of its high removal efficiency, low production cost, and wide availability. Effective Cr(VI) removal is achieved in an acidic solution using biochar derived from various feedstocks such as banana peduncle [12], sugar beet tailing [1], rice straw [13], municipal sludge [14], walnut hull [15], eucalyptus bark [16], and wheat straw and wicker [17]. Mohan et al. [30] proved effective remediation of Cr(VI)-contaminated water from 10 to 4 and 2.5 mg L^{-1} with 60% and 75% of Cr(VI) removal using oak wood and oak char, respectively; the removal mechanism was not investigated. In addition, few reviews have focused on the ability of oak wood biochar to release the cations Ca^{2+}, Na^{+}, and K^{+} to the treatment system at a low pH.

This study evaluated the effectiveness of using an oak wood biochar to remove aqueous Cr(VI); various techniques were utilized to characterize the oak wood biochar. The concentrations of cations and equilibrium pH were also measured to elucidate the removal mechanism. This study primarily aimed to (1) prove the feasibility of an oak wood biochar to treat aqueous Cr(VI) contamination; (2) summarize the influences of experimental factors, including pH value, reaction time, and initial concentration of Cr(VI); (3) evaluate the potential of biochar to release cations such as Ca^{2+}, Na^{+}, and K^{+} at pH 2.0; (4) elucidate the mechanism governing aqueous Cr(VI) removal.

2. Experimental section

2.1. Biochar characterization

Prior to use, oak wood biochar produced at ~700°C and purchased from Cowboy Charcoal Co. (TN, USA) was manually smashed and then sieved to particle size of 0.5–2 mm. Then, it was washed eight times with ultra-pure H_2O and vacuum-dried at 50°C for 24 h for future use. The surface area and pore volume were determined using a Bruanuer–Emmett–Teller (BET) analyzer (ASAP 2020). Biochar surface structure was observed via SEM (JEOL, JSM-5600, Japan) using an EDS to determine the inorganic constituents on the surface of the biochar. The surface functional groups were characterized using a Thermo Fisher, Nicolet iS5 instrument (USA) by performing FTIR analysis from 400 to 4,000 cm^{-1}. An ESCALAB 250 XPS with an Al K-Alpha spectrometer (Thermo Fisher Scientific, USA) was used to investigate the chemical composition precipitated onto the biochar. XPS analysis referenced the C1s binding energy corresponding to 284.6 eV to correct the data. In addition, the biochar pH_{zpc} was measured by a Zeta Sizer (Nano Series, Malvern Instruments, UK) at various pH 2.0–10.0.

2.2. Batch experiments

With the exception of concentrated nitric acid, which was guaranteed reagent grade (65%–68%), the chemicals used were of analytical grade. A solution was prepared in simulated groundwater (SMG: $CaCO_3$-saturated deionized water [18]) or deionized water. Cr(VI) stock solution (1 g L^{-1}) was obtained using $K_2Cr_2O_7$ powder (Beijing Reagent Co. Ltd., Beijing, China) dissolved in $CaCO_3$-saturated deionized water. Concentrated HNO_3 (16 M) (Sinopharm Chemical Reagent Co. Ltd., Shanghai, China) and 0.2 M NaOH (Beijing Reagent Co. Ltd., Beijing, China) were used for pH adjustment. Reaction samples were prepared by mixing 40 mL of Cr(VI)-spiked SMG with 0.4 g of biochar in 50 mL of polypropylene centrifuge tubes (Rotest Co. Ltd., Haimen, China). Samples containing only SMG, 50 mg L^{-1} of Cr (VI)-spiked SMG without biochar and 40 mL of plain SMG containing 0.4 g of biochar were used as controls to track the background contamination. All the reaction and control sample bottles were then agitated for 7 d at 120 rpm at room temperature (25°C ± 2°C). Experiments were conducted under aerobic conditions.

For the kinetic experiment, 0.4 g of biochar was blended into 40 mL of 50 mg L^{-1} Cr(VI) solution at pH 2.0. The influence of the initial pH on the removal experiment was determined at pH values of 2.0, 4.0, 6.0, and 8.1, maintaining the same concentrations of Cr(VI) and biochar as in the kinetic experiment. A dependence of initial concentration test was determined using Cr(VI) of 1.0, 5.0, 10, 25, 50, 100, 200, 400, and 600 mg L^{-1}, with 0.4 g of biochar at a fixed pH 2.0. A control experiment was also conducted to determine the possibility of Cr(III) removal. Supernatant samples were withdrawn at a specific time; these were then filtered using 0.22 μm Jinteng polyether sulfone membrane filters purchased from Tianjin of China, and the pre-experiments verified that the filters had a negligible impact on Cr sorption. All filtered liquid were preserved at 4°C prior to analyses. Duplicate tests were performed for all reactions and control samples to ensure accuracy.

2.3. Analytical methods

Total Cr was measured using a Shimadzu AA-6000CF atomic absorption spectrophotometer (Japan). A DR3900 spectrophotometer (Hach, USA) was utilized to quantify Cr(VI) concentration at 540 nm [19]. Cations concentrations were measured via ICP-MS (Agilent 7500C, USA). The system pH was determined using an Orion Star A221 pH meter, and its performance was verified using buffers of pH 7.0, 4.0, and 10.0 between samples.

2.4. Kinetics

The removal capacity (q, mg g^{-1}) of Cr(VI) by biochar was evaluated as follows:

$$q = V\frac{C_0 - C_e}{m} \tag{1}$$

where C_0 and C_e denote initial and residual concentration (mg L^{-1}), V is solution volume (mL), and m refers to biochar mass (g).

Cr(VI) removal was described using five frequently applied kinetic models, and rate equations (Eqs. (1)–(5)) are expressed as follows:

The pseudo-first-order kinetic (PFOK) model is represented as follows:

$$\ln\left(q_e - q_t\right) = \ln q_e - k_1 t \tag{2}$$

The pseudo-second-order kinetic (PSOK) model is represented as follows:

$$\frac{t}{q_t} = \frac{1}{k_2 q_e^2} + \frac{t}{q_e} \tag{3}$$

The intra-particle diffusion (IPD) model [20] is represented as follows:

$$q_t = k_3\, t^{0.5} \tag{4}$$

The modified Freundlich model [21] is represented as follows:

$$q_t = k_4 C_0 t^{1/m} \tag{5}$$

The Elovich model [22] is represented as follows:

$$q_t = \left(\frac{1}{\beta}\right)\ln(\alpha\beta) + \left(\frac{1}{\beta}\right)\ln t \tag{6}$$

where q_e and q_t (mg g^{-1}) are the treated Cr(VI) mass per unit mass of biochar at the terminal point and time t (h), respectively; k_1 (L h^{-1}), k_2 (g mg^{-1} h^{-1}), k_3 (mg g^{-1} h$^{-1/2}$), and k_4 (L g^{-1} h^{-1}) are, respectively, related to the rate constants of PFOK, PSOK, IPD, and the modified Freundlich; α (mg g^{-1} h^{-1}) and β (g mg^{-1}) are the Elovich constants; and m is the modified Freundlich constant.

3. Results and discussion

3.1. Removal kinetics

Cr(VI) was rapidly reduced within the first 60 min; more than 50% of aqueous Cr(VI) was removed possibly because of a rapid combination of Cr(VI) with the biochar surface (Fig. 1). The reaction rate then gradually decreased until equilibrium was achieved after 24 h; the maximum Cr(VI) removal percentage was 99.9%. The decrease in the reaction rate could be mainly due to the diffusion of Cr(VI) into the pores of the biochar [15,23].

The kinetic data were fitted to five kinetic models to determine the Cr(VI) removal mechanism. The plots are depicted in Figs. 2 and S1. As presented in Table 1, the regression coefficients (R^2) were 0.9999, 0.8539, 0.7772, 06669, and 0.5939 for PSOK, Elovich, modified Freundlich, PFOK, and IPD models, respectively. Results revealed that the kinetic data better fitted with the PSOK model than with the other four equations; this finding was in agreement with published studies [24]. The high value of R^2 may be due to the chemical process, such as chemisorption, involving valence force through electron transfer between Cr(VI) and the biochar [25].

3.2. Effect of pH

The maximum Cr(VI) removal was 99.9% which was observed at pH 2.0 (Fig. 3). Cr(VI) removal sharply declined as the solution pH was raised from pH 2.0 to 8.1, eventually decreasing to 0%. Similarly, a decline in Cr(VI) removal resulting from an increase in pH was also observed in other findings [1,15,26,27]. Choudhary et al. [16] reported that Cr(VI) removal decreases as the pH (>4.0) increases with pH 2.0 being the optimal condition. Furthermore, Dong et al. [1] illustrated that complete Cr(VI) treatment occurred when at pH 2.0 compared with 16% removal at pH 3.0. A considerable decrease in Cr(VI) removal as pH increases may be attributed to the increased hindrance of Cr(VI) adsorbed on biochar by OH^-. At a low pH (2.0), Cr(VI) removal was higher possibly because Cr ions (negatively charged) migrated to the protonated biochar surface under the strong electrostatic force.

Cr(VI) in solution is in the stable forms of $Cr_2O_7^-$, $HCrO_4^-$, $Cr_3O_{10}^{2-}$, and $Cr_4O_{13}^{2-}$; $HCrO_4^-$ was the predominant species in the solution at pH < 6.1 [28]. As shown in Fig. 3b, the pH_{zpc} of biochar was 3.36. The surface charge of the biochar was positive for pH < pH_{zpc}; otherwise, the biochar surface was negatively charged [29], which could inhibit Cr(VI) from adsorbing on its surface. At pH 2.0, the presence of numerous

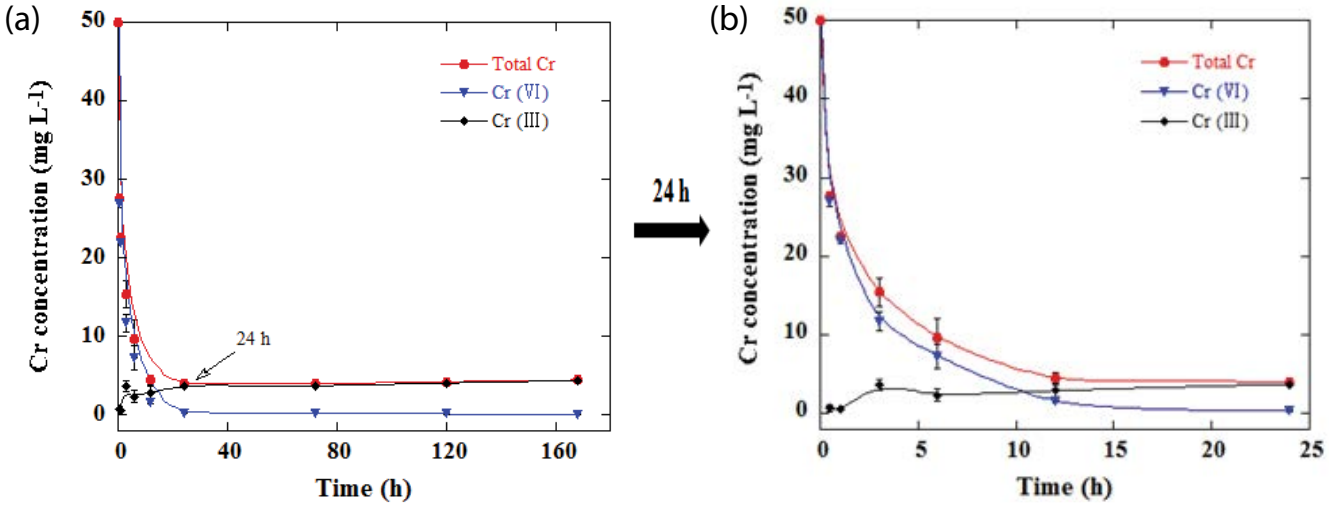

Fig. 1. Effect of reaction time on Cr(VI) removal (initial Cr(VI) concentration: 50 mg L^{-1}, dose of biochar: 10 g L^{-1}, solution pH: 2.0).

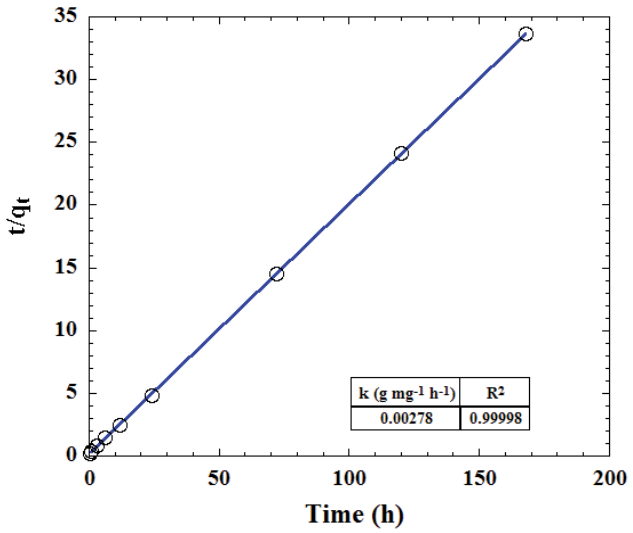

Fig. 2. Kinetic fitting plots of the pseudo-second-order equation for Cr(VI) removal (initial Cr(VI) concentration: 50 mg L^{-1}, dose of biochar: 10 g L^{-1}, solution pH: 2.0).

aqueous H^+ ions created a strong positively charged biochar; an electrostatic interaction formed between the positively charged biochar and the negatively charged Cr(VI) ions. At pH > 4.0, negligible removal of Cr(VI) was likely attributable to electrostatic repulsion. In addition, the transformation of Cr(VI) to Cr(III) was observed in strongly acidic conditions [30,31]. Therefore, the following tests were conducted at the optimal pH of 2.0.

3.3. Effect of initial Cr(VI) concentration

Cr(VI) removal capacity of biochar was greatly affected by the initial concentration of Cr(VI) (Fig. 4). More than 99.9% of initial Cr(VI) (<50 mg L^{-1}) was removed; however, Cr(VI) removal efficiency and biochar performance decreased from 99.9% at 4.99 mg g^{-1} of biochar to 0% at 0.05 mg g^{-1} of biochar whereas Cr(VI) was within 50–600 mg L^{-1}. The reduction in removal that appeared with increased initial Cr(VI) concentration was probably caused by the decreasing available sorption sites of the biochar [1]. Overall, the removal capacity was considerably Cr(VI) concentration-dependent within a certain range (50–600 mg L^{-1}), but it remained constant at 4.99 mg g^{-1} at low Cr(VI) concentrations.

3.4. SEM/EDS and BET analysis

SEM images and EDS spectra of biochar are presented in Fig. 5. Smooth surfaces and porous structures were observed on the raw material (Fig. 5a). In contrast, rough surfaces with a thick layer of tiny particles were observed on the biochar after reacting to Cr(VI) (Fig. 5b). In addition, the obvious Cr

Table 1
Parameters of different kinetic models fitted to the Cr(VI) removal by biochar

	Pseudo-first-order	Pseudo-second-order	IPD	Modified Freundlich	Elovich
k	0.04174 L h^{-1}	0.00278 g mg^{-1} h^{-1}	0.01126 mg g^{-1} $h^{-1/2}$	0.05938 L g^{-1} h^{-1}	–
m	–	–	–	7.8796	–
α	–	–	–	–	332.2637 mg g^{-1} h^{-1}
β	–	–	–	–	2.1519 g mg^{-1}
R^2	0.6669	0.9999	0.5939	0.7772	0.8539

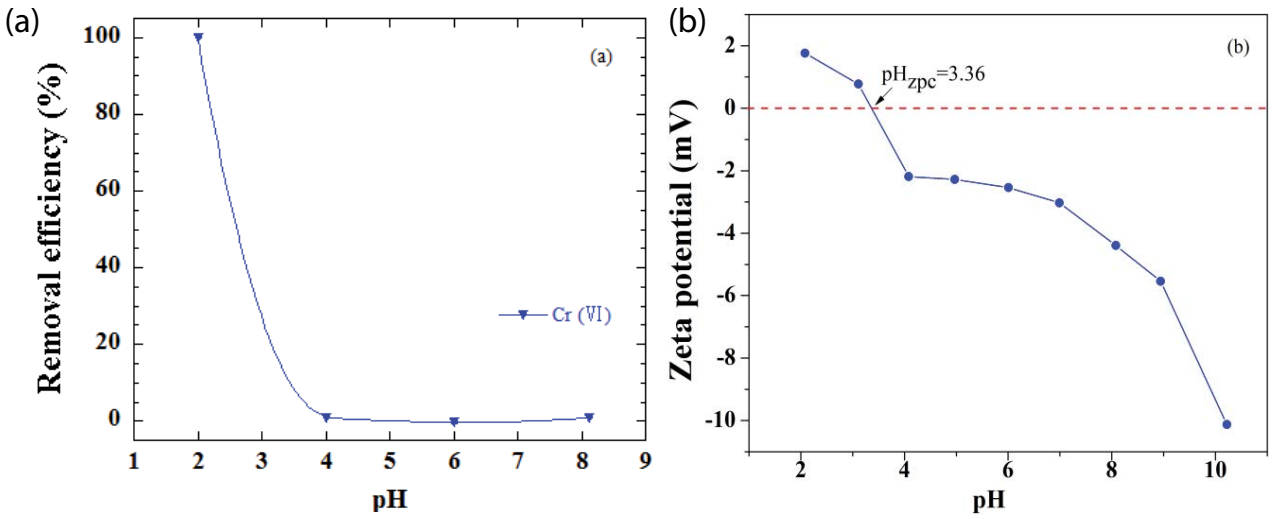

Fig. 3. (a) Effect of solution pH on Cr(VI) removal (initial Cr(VI) concentration: 50 mg L^{-1}, dose of biochar: 10 g L^{-1} reaction time: 168 h and (b) zeta potential of oak biochar at different solution pH.

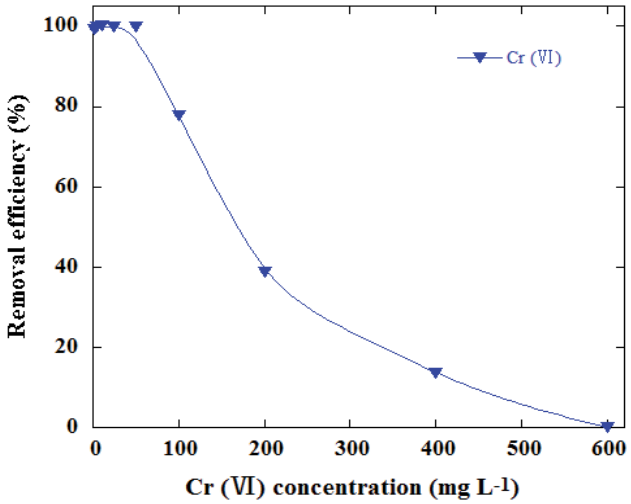

Fig. 4. Effect of initial Cr(VI) concentration on removal efficiency at pH 2.0 (dose of biochar = 10 g L^{-1}, reaction time: 168 h, solution pH: 2.0).

peak observed in the corresponding EDS spectra (Fig. 5d) after the reaction confirmed Cr adsorption on the biochar. A portion of the available sorption sites was occupied after Cr combined with the biochar through adsorption and complexation; this may lead to decreases in pore volume and surface area (Table S1).

3.5. Fourier transform infrared spectroscopy analysis

Abundant adsorption peaks were observed (Fig. 6), which revealed the complex functional groups of biochar. A characteristic peak at ~3,440 cm^{-1} was denoted to –OH groups (2,500–3,500 cm^{-1}) [32], and typical bands of 2,920 and 1,384 cm^{-1} corresponded with the C–H stretching vibration group [33,34]. A band at 1,724 cm^{-1} indicated the existence of O=C–O functional groups, which may bind with Cr(III) reduced from Cr(VI) [13]. A band at ~1,629 cm^{-1} was also observed, which corresponded to the aromatic C=C or carboxylic C=O chelate stretching [16,35]. Absorbance bands near 1,078 and 1,046 cm^{-1} likely indicated the C–O bending vibration of alcoholic groups [1]. After Cr(VI) treatment,

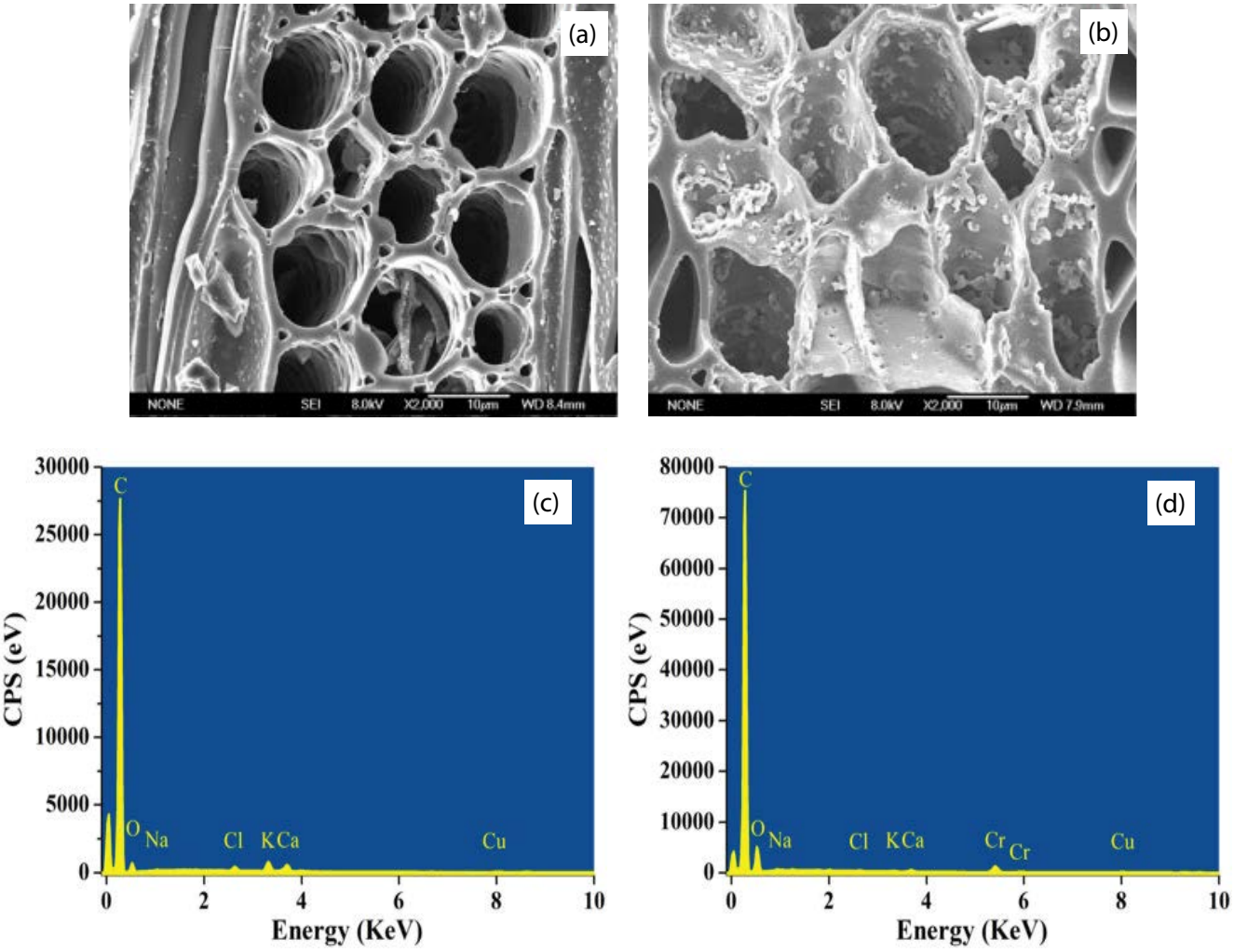

Fig. 5. SEM images of biochar (a) before and (b) after treatment with Cr(VI); EDS spectrum of biochar (c) before and (d) after treatment with Cr(VI) (initial Cr(VI) concentration: 50 mg L^{-1}, dose of biochar: 10 g L^{-1}, reaction time: 168 h, solution pH: 2.0).

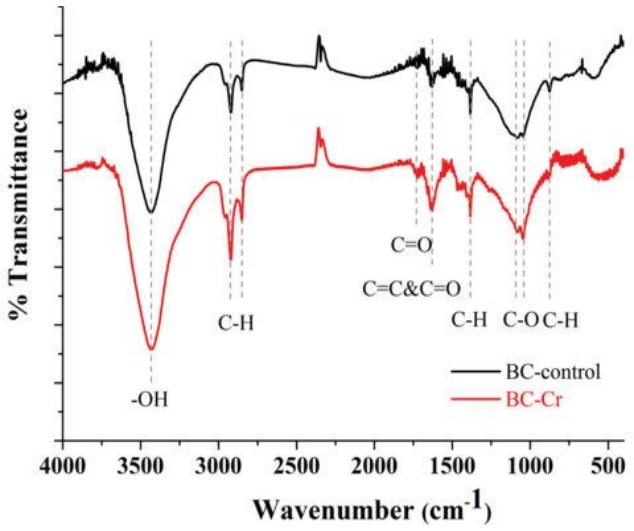

Fig. 6. Fourier transformation infrared spectra of biochar before and after treatment with 50 mg L^{-1} Cr(VI) after 168 h at pH 2.0.

various functional groups of biochar could be observed. C–H and C=C peaks increased in intensity. C–O peak became sharper, and the intensities of the C=O group increased. These two changes occurred because the C–O band was oxidized by Cr(VI) and formed a new C=O group that could bind with Cr(III) ions [13]. Variations in Fourier transform infrared spectroscopy (FTIR) spectra confirmed that C=C, C–H, C–O, and C=O may play a vital role in Cr(VI) treatment.

3.6. XPS analysis

After Cr(VI) was loaded on the biochar, the C1s and O1s spectra of biochar considerably varied (Fig. 7). The XPS C1s spectra were curve-fitted to five peaks, which were attributed to different species of the surface components (Figs. 7a and b). The peaks at 284.0, 284.8, and 284.4 eV corresponded with C=C, C–C (sp^2–hybridized C), and C–C (sp^3–hybridized C) bonds [36,37], respectively. A characteristic band at 285.4 eV represented the C–O bonds (phenolic, alcohol, or ether groups) [16] and the peaks at 288.1 and 286.2 eV corresponded to C=O and C–O–C bonds [29], respectively. Relative percentages of functional groups changed after equilibration with Cr(VI). C–O decreased from 12.93% to 11.67%, and C–O–C reduced from 17.09% to 10.98%; however, the C=O groups increased from 9.25% to 9.85% (Table 2).

The O1s regions of raw biochar and Cr(VI)-loaded biochar are shown in Figs. 7c and d. Three peaks were observed in the O1s spectra of raw biochar including C=O (530.9 eV), O–C=O (533.0 eV), and C–O bonds (532.9 eV) [16,38]. Four peaks were observed in the O1s spectra of Cr-loaded biochar. C=O in Cr(VI)–loaded biochar increased from 40.10% to 43.37%; meanwhile, the relative content of C–O and O–C=O decreased to 9.36% and 15.50%, respectively. These phenomena are possibly caused by C–O and C–O–C oxidation by Cr(VI), generating C=O [28]. A $Cr(OH)_3$ peak appeared at 531.02 eV [39] indicating the transformation of Cr(VI) to Cr(III) during treatment. Overall, C–O and C–O–C bands on biochar greatly contributed to Cr(VI) removal.

Fig. 7e illustrates the Cr 2p spectrum after the reaction. The spectrum had two peaks corresponding to Cr $2p_{1/2}$ (586.9 eV) and Cr $2p_{3/2}$ (577.2 eV) [16]. The Cr 2p spectrum showed that the coexistence of hexavalent and trivalent Cr with biochar and Cr(III) species occupied a large proportion of Cr. The peaks of 576.7 and 577.8 eV were regarded as Cr_2O_3 and $Cr(OH)_3$ [17], which presented about ~21.40% and 61.56%, respectively. Furthermore, the band of 579.2 eV, which corresponded to Cr(VI) [40] only accounted for 17.04%. These findings illustrated that incomplete Cr(VI) reduction occurred after 168 h. The results identified from XPS were coincident with previous FTIR studies showing that Cr(VI) removal involves surface functional groups of biochar.

Table 2
Components of C 1s, O 1s and Cr 2p for the XPS spectra and their relative percentage for the biochar before and after reaction with Cr(VI)

	Components	Relative percentage (%)		Binding energy (eV)	
		Before	After	Before	After
C 1s	C=C	11.44	14.74	284.0	284.0
	C–C (sp^2-carbon)	24.56	19.22	284.4	284.4
	C–C (sp^3-carbon)	24.73	33.54	284.8	284.8
	C–O	12.93	11.67	285.4	285.4
	C–O–C	17.09	10.98	286.2	286.2
	C=O	9.25	9.85	288.1	288.3
O 1s	C=O	40.10	43.37	531.5	531.6
	O–C=O	34.49	18.99	532.6	532.4
	C–O	25.40	16.04	533.5	533.6
	O–Cr	–	21.60	–	531.0
Cr 2p	Cr_2O_3	–	21.40	–	576.7
	$Cr(OH)_3$	–	61.56	–	577.8
	Cr(VI)	–	17.04	–	579.2

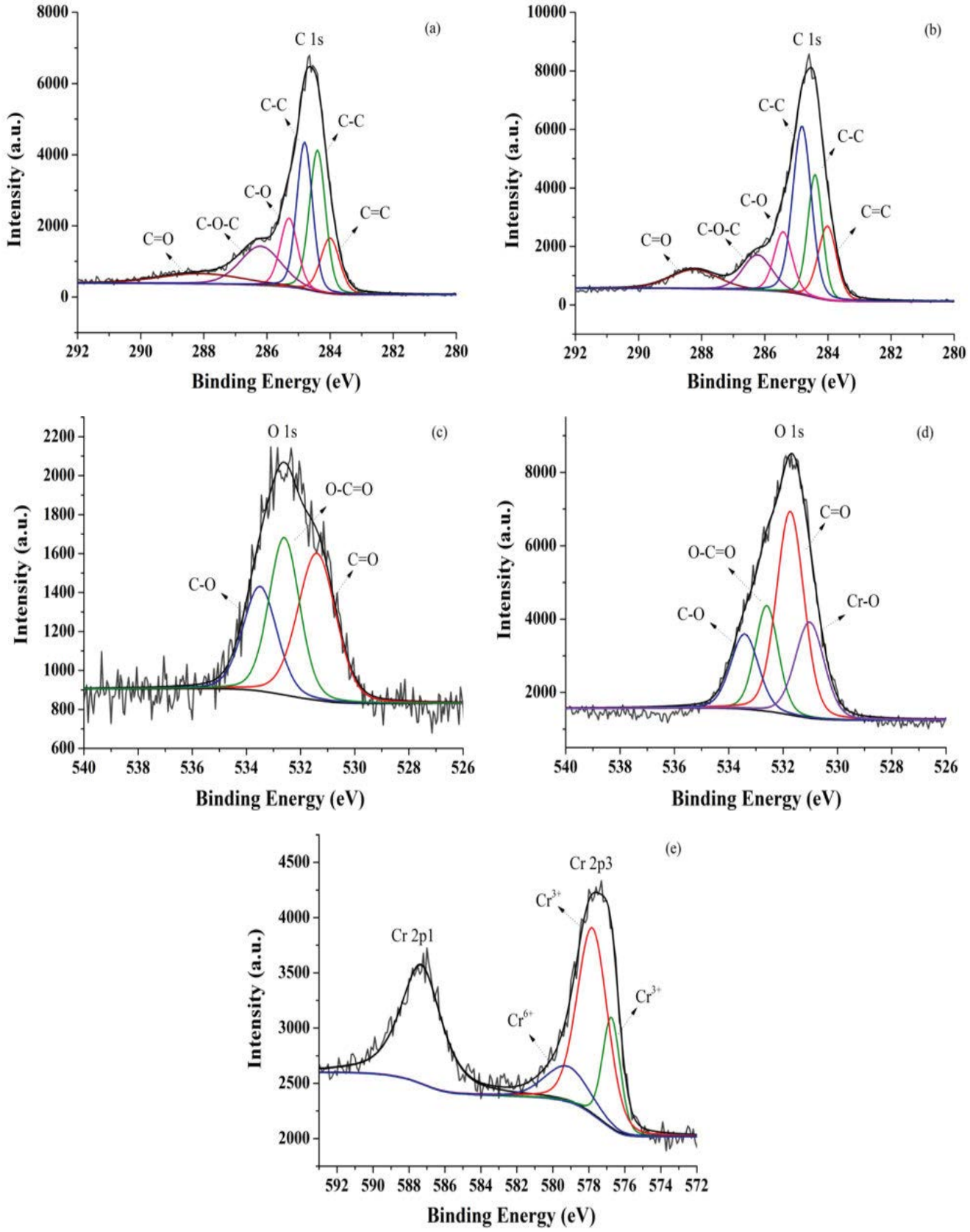

Fig. 7. High resolution XPS spectra of C 1s ((a) before and (b) after reaction), O 1s ((c) before and (d) after Cr(VI) reaction) and Cr 2p (e) after reaction.

Table 3
Cation concentrations in solutions before and after reaction with 50 mg L^{-1} Cr(VI) at pH 2.0 after 7 d

Cations	Before reaction (mg L^{-1})	After reaction (mg L^{-1})	Only SMG (mg L^{-1})	Only 50 mg L^{-1} Cr(VI) spiked-SMG (mg L^{-1})	MDLs (mg L^{-1})
Na	12.5	17.4	0.31	5.06	0.006
Mg	2.93	1.59	1.25	0.42	0.002
Al	0.64	<MDL	0.66	<MDL	0.001
K	56.9	115	7.93	57.8	0.005
Ca	133	253	51.4	165	0.007
Cr	0.04	4.29	0.02	52.4	0.0001
Fe	3.81	0.72	4.00	<MDL	0.0008
Cu	0.26	<MDL	0.21	<MDL	0.00008
Zn	0.15	0.17	0.15	0.11	0.0007
Sr	7.62	6.11	0.21	0.08	0.0003
Ba	1.11	1.28	0.12	0.17	0.0002

Note: MDLs-Method detection limits of cations.

3.7. Removal mechanisms of Cr(VI) by oak wood biochar

FTIR results indicated the presence of abundant biochar in the functional groups, including O–H, C=C, C–O, C=O, and C–H. Some functional group peaks considerably changed after Cr(VI) removal (Fig. 6). Moreover, XPS investigation confirmed that Cr(III) was the predominant form on Cr-loaded biochar, and C–O groups of biochar reduced a large proportion of Cr(VI). After equilibrium, concentrations of cations such as Ca^{2+}, Na^{+}, and K^{+} in the reaction system increased (Table 3) and the final pH increased to 3.0. The increase in cation concentrations and pH indicated that ion exchange might be another decisive factor for Cr(III) binding to the biochar. The Cr(VI) removal mechanism comprised the following three steps: (1) Cr(VI) was attracted to the protonated surface of the biochar through electrostatic interaction at pH 2.0; (2) a large proportion of attached Cr(VI) ions were subsequently converted to Cr(III) by C–O from alcoholic groups (Fig. 7e); and (3) the reduced Cr(III) was partially combined with the biochar via ion exchange and complexation, and then the remainder got rid of the biochar to the solution under the effect of electronic repulsion. Thus, Cr(VI) treatment by oak wood biochar was a combination of adsorption and reduction.

4. Conclusions

Results revealed the effectiveness of low-cost oak wood biochar for aqueous Cr(VI) treatment. The reaction reflected high dependence on pH and the initial concentration of Cr(VI). The maximum Cr(VI) removal percentage achieved was 99.9% at a low pH value of 2.0. Cr(VI) could be entirely removed at a concentration of 1–50 mg L^{-1}; however, the removal capacity of the biochar reduced as Cr(VI) concentration increased. The removal of Cr(VI) using oak wood biochar followed the PSOK model ($R^2 > 0.9999$). Various FTIR spectra verified that C–O groups of alcohol and C=O groups may be involved in Cr(VI) treatment using biochar. The transformation of hexavalent Cr to trivalent Cr after Cr(VI) was attracted to the biochar was further proved by XPS results. The reaction was considered to be a combination of multiple procedures, including electrostatic force between hexavalent Cr and the biochar, hexavalent Cr reduction, and ion exchange between Cr(III) and the cations, and complexation between Cr(III) and the C=O group on the biochar. Overall, the oak wood biochar exhibited good latent capacity for aqueous Cr(VI) treatment under acidic pH.

Acknowledgements

This study was supported by the National Natural Science Foundation of China (41572217) and the 111 Project (B16020) of China.

References

[1] X. Dong, L.Q. Ma, Y. Li, Characteristics and mechanisms of hexavalent chromium removal by biochar from sugar beet tailing, J. Hazard. Mater., 190 (2011) 909–915.
[2] X. Huang, Y. Liu, S. Liu, X. Tan, Y. Ding, G. Zeng, Y. Zhou, M. Zhang, S. Wang, B. Zheng, Effective removal of Cr(VI) using β-cyclodextrin–chitosan modified biochars with adsorption/reduction bifuctional roles, RSC Adv., 6 (2016) 94–104.
[3] J. Kotaś, Z. Stasicka, Chromium occurrence in the environment and methods of its speciation, Environ. Pollut., 107 (2000) 263–283.
[4] D. Mohan, K.P. Singh, V.K. Singh, Removal of hexavalent chromium from aqueous solution using low-cost activated carbons derived from agricultural waste materials and activated carbon fabric cloth, Ind. Eng. Chem. Res., 44 (2005) 1027–1042.
[5] D. Mohan, C.U. Pittman Jr., Activated carbons and low cost adsorbents for remediation of tri- and hexavalent chromium from water, J. Hazard. Mater., 137 (2006) 762–811.
[6] A. Baral, R.D. Engelken, Chromium-based regulations and greening in metal finishing industries in the USA, Environ. Sci. Policy, 5 (2002) 121–133.
[7] A. Özer, H.S. Altundoğan, M. Erdem, F. Tümen, A study on the Cr(VI) removal from aqueous solutions by steel wool, Environ. Pollut., 97 (1997) 107–112.
[8] S. Chakraborty, J. Dasgupta, U. Farooq, J. Sikder, E. Drioli, S. Curcio, Experimental analysis, modeling and optimization of chromium (VI) removal from aqueous solutions by polymer-enhanced ultrafiltration, J. Membr. Sci., 456 (2014) 139–154.
[9] L. Alvarado, I.R. Torres, A. Chen, Integration of ion exchange and electrodeionization as a new approach for the continuous

treatment of hexavalent chromium wastewater, Sep. Purif. Technol., 105 (2013) 55–62.
[10] X. Ren, C. Zhao, S. Du, T. Wang, Z. Luan, J. Wang, D. Hou, Fabrication of asymmetric poly (*m*-phenylene isophthalamide) nanofiltration membrane for chromium(VI) removal, J. Environ. Sci., 22 (2010) 1335–1341.
[11] M.D. Afonso, J.O. Jaber, M.S. Mohsen, Brackish groundwater treatment by reverse osmosis in Jordan, Desalination, 164 (2004) 157–171.
[12] A.A. Karim, M. Kumar, S. Mohapatra, C.R. Panda, A. Singh, Banana peduncle biochar: characteristics and adsorption of hexavalent chromium from aqueous solution, Int. Res. J. Pure Appl. Chem., 7 (2015) 1–10.
[13] N.-H. Hsu, S.-L. Wang, Y.-H. Liao, S.-T. Huang, Y.-M. Tzou, Y.-M. Huang, Removal of hexavalent chromium from acidic aqueous solutions using rice straw-derived carbon, J. Hazard. Mater., 171 (2009) 1066–1070.
[14] T. Chen, Z. Zhou, S. Xu, H. Wang, W. Lu, Adsorption behavior comparison of trivalent and hexavalent chromium on biochar derived from municipal sludge, Bioresour. Technol., 190 (2015) 388–394.
[15] X.S. Wang, Z.Z. Li, S.R. Tao, Removal of chromium (VI) from aqueous solution using walnut hull, J. Environ. Manage., 90 (2009) 721–729.
[16] B. Choudhary, D. Paul, A. Singh, T. Gupta, Removal of hexavalent chromium upon interaction with biochar under acidic conditions: mechanistic insights and application, Environ. Sci. Pollut. Res. Int., 24 (2017) 16786–16797.
[17] A. Tytłak, P. Oleszczuk, R. Dobrowolski, Sorption and desorption of Cr(VI) ions from water by biochars in different environmental conditions, Environ. Sci. Pollut. Res. Int., 22 (2015) 5985–5994.
[18] D.W. Blowes, C.J. Ptacek, J.L. Jambor, *In-situ* remediation of Cr(VI)-contaminated groundwater using permeable reactive walls: laboratory studies, Environ. Sci. Technol., 31 (1997) 3348–3357.
[19] C.E. Turick, W.A. Apel, A bioprocessing strategy that allows for the selection of Cr(VI)-reducing bacteria from soils, J. Ind. Microbiol. Biotechnol., 18 (1997) 247–250.
[20] D. Kołodyńska, R. Wnętrzak, J.J. Leahy, M.H.B. Hayes, W. Kwapiński, Z. Hubicki, Kinetic and adsorptive characterization of biochar in metal ions removal, Chem. Eng. J., 197 (2012) 295–305.
[21] N. Liu, A.B. Charrua, C.-H. Weng, X. Yuan, F. Ding, Characterization of biochars derived from agriculture wastes and their adsorptive removal of atrazine from aqueous solution: a comparative study, Bioresour. Technol., 198 (2015) 55–62.
[22] M. Inyang, B. Gao, Y. Yao, Y. Xue, A.R. Zimmerman, P. Pullammanappallil, X. Cao, Removal of heavy metals from aqueous solution by biochars derived from anaerobically digested biomass, Bioresour. Technol., 110 (2012) 50–56.
[23] A. Jang, Y. Seo, P.L. Bishop, The removal of heavy metals in urban runoff by sorption on mulch, Environ. Pollut., 133 (2005) 117–127.
[24] M. Aliabadi, I. Khazaei, H. Fakhraee, M.T.H. Mousavian, Hexavalent chromium removal from aqueous solutions by using low-cost biological wastes: equilibrium and kinetic studies, Int. J. Environ. Sci. Technol., 9 (2012) 319–326.
[25] Y.S. Ho, J.C.Y. Ng, G. McKay, Kinetics of pollutant sorption by biosorbents: review, Sep. Purif. Methods, 29 (2011) 189–232.
[26] V.K. Gupta, D. Mohan, S. Sharma, K.T. Park, Removal of chromium(VI) from electroplating industry wastewater using bagasse fly ash—a sugar industry waste material, Environmentalist, 19 (1998) 129–136.
[27] A.U. Rajapaksha, M.S. Alam, N. Chen, D.S. Alessi, A.D. Igalavithana, D.C.W. Tsang, Y.S. Ok, Removal of hexavalent chromium in aqueous solutions using biochar: chemical and spectroscopic investigations, Sci. Total Environ., 625 (2018) 1567–1573.
[28] W. Liu, J. Zhang, C. Zhang, L. Ren, Preparation and evaluation of activated carbon-based iron-containing adsorbents for enhanced Cr(VI) removal: mechanism study, Chem. Eng. J., 189–190 (2012) 295–302.
[29] B. Yousaf, G. Liu, Q. Abbas, R. Wang, H. Ullah, M.M. Mian, A. Rashid, Enhanced removal of hexavalent chromium from aqueous media using a highly stable and magnetically separable rosin-biochar-coated TiO_2@C nanocomposite, RSC Adv., 8 (2018) 25983–25996.
[30] D. Mohan, S. Rajput, V.K. Singh, P.H. Steele, C.U. Pittman Jr., Modeling and evaluation of chromium remediation from water using low cost bio-char, a green adsorbent, J. Hazard. Mater., 188 (2011) 319–333.
[31] X.S. Wang, L.F. Chen, F.Y. Li, K.L. Chen, W.Y. Wan, Y.J. Tang, Removal of Cr (VI) with wheat-residue derived black carbon: reaction mechanism and adsorption performance, J. Hazard. Mater., 175 (2010) 816–822.
[32] H. Zhang, X. Yue, F. Li, R. Xiao, Y. Zhang, D. Gu, Preparation of rice straw-derived biochar for efficient cadmium removal by modification of oxygen-containing functional groups, Sci. Total Environ., 631 (2018) 795–802.
[33] A. Kapoor, T. Viraraghavan, Heavy metal biosorption sites in *Aspergillus niger*, Bioresour. Technol., 61 (1997) 221–227.
[34] Z.-b. Zhang, X.-h. Cao, P. Liang, Y.-h. Liu, Adsorption of uranium from aqueous solution using biochar produced by hydrothermal carbonization, J. Radioanal. Nucl. Chem., 295 (2012) 1201–1208.
[35] C.H. Chia, B. Gong, S.D. Joseph, C.E. Marjo, P. Munroe, A.M. Rich, Imaging of mineral-enriched biochar by FTIR, Raman and SEM–EDX, Vib. Spectrosc., 62 (2012) 248–257.
[36] J.R. Araujo, B.S. Archanjo, K.R. De Souza, W. Kwapinski, N.P.S. Falcão, E.H. Novotny, C.A. Achete, Selective extraction of humic acids from an anthropogenic Amazonian dark earth and from a chemically oxidized charcoal, Biol. Fertil. Soils, 50 (2014) 1223–1232.
[37] W. Zhang, J. Cui, C.A. Tao, Y. Wu, Z. Li, L. Ma, Y. Wen, G. Li, A strategy for producing pure single-layer graphene sheets based on a confined self-assembly approach, Angew. Chem. Int. Ed., 48 (2009) 5864–5868.
[38] C.H. Cheng, J. Lehmann, J.E. Thies, S.D. Burton, M.H. Engelhard, Oxidation of black carbon by biotic and abiotic processes, Org. Geochem., 37 (2006) 1477–1488.
[39] S. Survilienė, R. Juškėnas, V. Jasulaitienė, A. Selskienė, A. Češūnienė, A. Suchodolskis, V. Karpavičienė, Annealing effect on the structural and optical properties of black chromium electrodeposited from the Cr(III) bath, Chemija, 26 (2015) 244–253.
[40] V. Murphy, S.A. Tofail, H. Hughes, P. McLoughlin, A novel study of hexavalent chromium detoxification by selected seaweed species using SEM-EDX and XPS analysis, Chem. Eng. J., 148 (2009) 425–433.

Supplementary Information

Table S1
BET characteristic of biochar before and after reaction with Cr(VI)

	Specific surface area ($m^2 g^{-1}$)	Pore volume ($m^3 g^{-1}$)	Pore size (nm)
Before	64.53	0.03562	2.20842
After	14.58	0.00670	1.83749

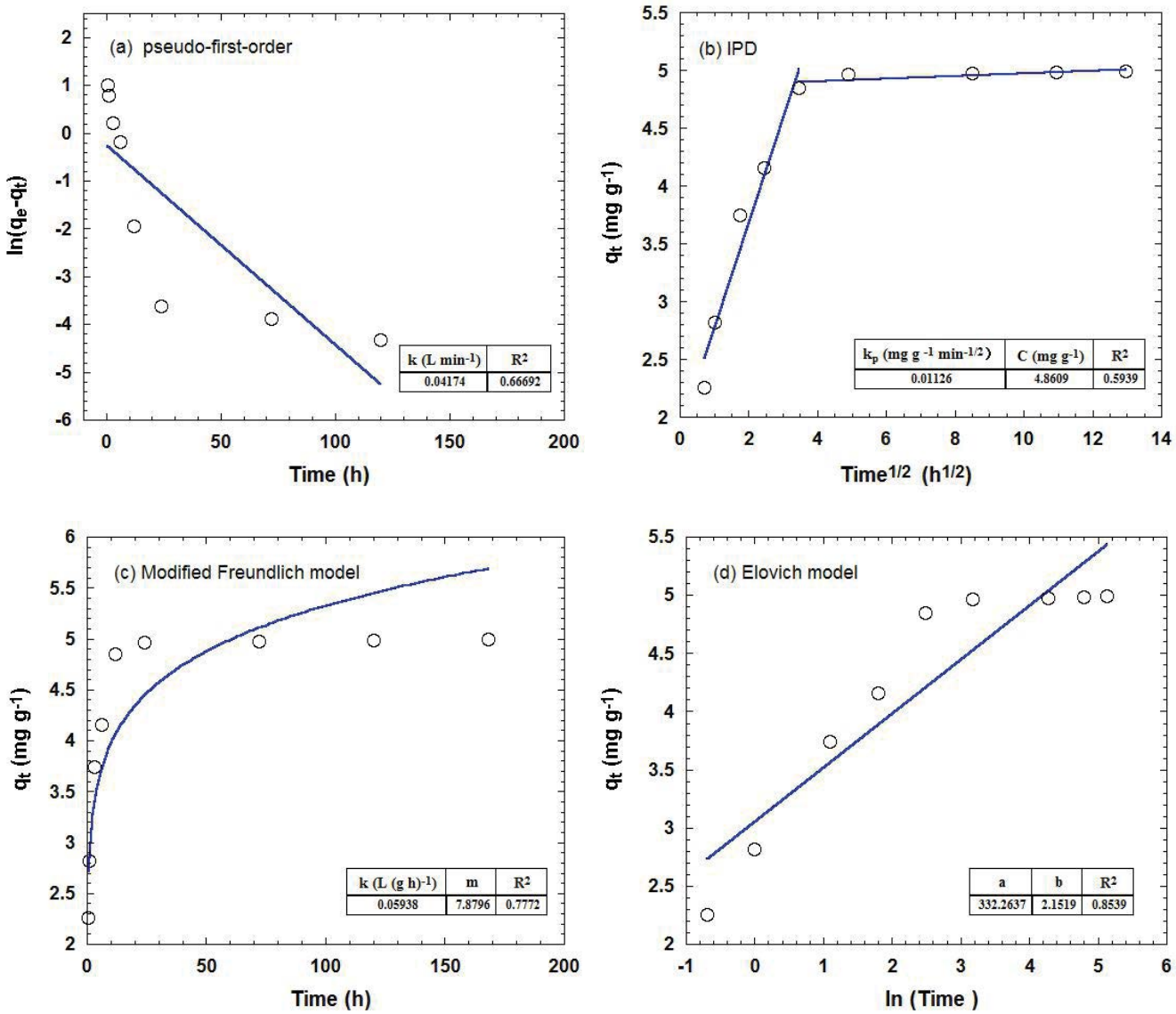

Fig. S1. Kinetic fitting plots of the (a) pseudo-first-order equation, (b) IPD equation, (c) modified Freundlich equation, and (d) Elovich equation.